Commun Nonlinear Sci Numer Simulat 15 (2010) 3640–3646

Contents lists available at ScienceDirect

Commun Nonlinear Sci Numer Simulat

journal homepage: www.elsevier.com/locate/cnsns

Suppression of pull-in instability in MEMS using a high-frequency actuation

Faouzi Lakrad *, Mohamed Belhaq

University Hassan II-Casablanca, BP 5366 Maarif, Casablanca, Morocco

ARTICLE INFO

Article history:
Received 21 August 2009
Received in revised form 25 December 2009
Accepted 27 December 2009
Available online 4 January 2010

Keywords:
Pull-in
MEMS
High-frequency voltage

ABSTRACT

We study the effect of a high-frequency AC tension on the pull-in instability induced by a DC tension in a microelectromechanical system. The microstructure is modelled as a single-degree-of-freedom system. The method of direct partition of motion is used to split the fast and slow dynamics. Analysis of steady-states of the slow dynamic enables us to depict the effect of the AC voltage on the pull-in. The main result of this paper indicates that it is possible to suppress the electrostatically induced pull-in instability for a range of values of the amplitude and the frequency of the high-frequency AC.

1. Introduction

Electrostatically actuated microelectromechanical systems (MEMS) find many applications today in areas such as inertial sensors, relays, switches, etc. A serious limitation on the use of these devices lies in the pull-in phenomenon [1–3], which is a structural instability resulting from the interaction between elastic and electrostatic forces. This instability results from the unbalance between the electric actuation and the mechanical restoring force leading the suspended microbeam to hit the stationary electrode underneath it causing stiction and short circuit problems and hence the failure in the device's function [4].

Keeping MEMS devices operating in a stable regime away from the pull-in instability limit has a crucial interest from design and commercialization point of view. Various works [5,6] investigated the static pull-in phenomenon and performed techniques to predict its occurrence by determining the largest DC voltage for which the system operate in a stable behavior. The dynamic pull-in was studied under various loads, for instance step voltage [7], AC harmonic voltage [8] and mechanical shock load [9]. It was shown that the dynamic actuation reduces drastically the static pull-in limit. In the framework of controlling the pull-in, a control method consisting in adding superharmonics to a reference harmonic excitation was proposed in [10]. In the present work, a high-frequency voltage (HFV) is used to suppress an initially established static pull-in. The proposed method is applied to a simplified mass-spring-damping system modelling the dynamic of capacitive MEMS. It is worth nothing that the problem of studying the effect of high-frequency excitation on the dynamic of mechanical systems has been examined previously by a number of authors; see for instance [11] and references therein. Recent works focused attention on the effect of high-frequency excitation on natural frequencies [12,13], symmetry breaking [14], on limit cycles [15] and on hysteresis [16,17]. The rest of the paper is organized as follows: In Section 2, after describing the model, an averaging technique is performed over the rapid dynamic produced by HFV and an equation governing the slow dynamic of the MEMS device is derived. In Section 3, the effect of a HFV on the occurrence of the pull-in instability is investigated. Section 4 concludes the work.

* Corresponding author.
E-mail address: lakrad@hotmail.com (F. Lakrad).

1007-5704/$ - see front matter © 2010 Elsevier B.V. All rights reserved.
doi:10.1016/j.cnsns.2009.12.033

2. Formulation of the problem and the slow dynamic

A single-degree-of-freedom model depicted in Fig. 1 is utilized to represent a capacitive MEMS device employing a DC and AC voltages as actuator.

$$m\ddot{x} + c\dot{x} + kx = \frac{\varepsilon A}{2(d-x)^2}V^2 \tag{1}$$

where x is the displacement of the movable mass m, c and k are the damping and stiffness of the system, respectively. The dielectric constant of the gap medium is denoted ε, d is the initial capacitor gap width, A is the area of the cross section, and V is the electric load.

The tension is given by the following AC and DC voltages:

$$V = V_0 + U\cos(\Omega^* t) \tag{2}$$

where V_0 is a DC voltage, whereas U and Ω^* are the amplitude and the frequency of the AC actuation, respectively.

The square of this tension is given by

$$V^2 = \left(V_0^2 + \frac{U^2}{2}\right) + 2V_0U\cos(\Omega^* t) + \frac{U^2}{2}\cos(2\Omega^* t) \tag{3}$$

Thus, the AC tension contributes positively in the electrostatic force acting on the movable electrode. As a consequence, the static pull-in threshold is affected. In order to preclude this effect, a new DC tension V_1 is added and it is chosen to vanish this undesirable contribution. Thus the electric tension can be written as follows:

$$V = V_0 + V_1 + U\cos(\Omega^* t) \tag{4}$$

with $V_1 = -V_0 \pm 0.5\sqrt{4V_0^2 - 2U^2}$. It is worth noting that V_1 exists only for $U \leqslant \sqrt{2}V_0$. Consequently, the square of the tension is given by

$$V^2 = V_0^2 \pm U_1^2\cos(\Omega^* t) + U_2^2\cos(2\Omega^* t) \tag{5}$$

where $U_1^2 = U\sqrt{4V_0^2 - 2U^2}$ and $U_2^2 = U^2/2$. We set $X = \frac{x}{d}$, $\tau = \omega t$, $\omega = \sqrt{\frac{k}{m}}$, $\xi = \frac{c}{2m\omega}$ and $\Omega = \frac{\Omega^*}{\omega}$. Thus the nondimensional equation of motion is given by

$$X'' + 2\xi X' + X = \frac{\alpha}{(1-X)^2} + \frac{\beta}{(1-X)^2}\cos(\Omega\tau) + \frac{\gamma}{(1-X)^2}\cos(2\Omega\tau) \tag{6}$$

The primes denote the derivatives with respect to the normalized time τ, and

$$\alpha = \frac{\varepsilon A}{2m\omega^2 d^3}V_0^2 \tag{7}$$

$$\beta = \pm\frac{\varepsilon A}{2m\omega^2 d^3}U_1^2 \tag{8}$$

$$\gamma = \frac{\varepsilon A}{2m\omega^2 d^3}U_2^2 \tag{9}$$

These coefficients are related by the following expression:

$$\beta^2 = 8\gamma(\alpha - \gamma) \tag{10}$$

When fixing two parameters of the electric actuation the third one is determined. Fig. 2 shows β versus γ for various values of α. The allowed parameters in the plane $(\beta,\ \gamma)$ constitute symmetric ellipsis, with respect to β, that are increasing when the electrostatic effect α increases. The upper bound value of this latter is given by the pull-in instability threshold.

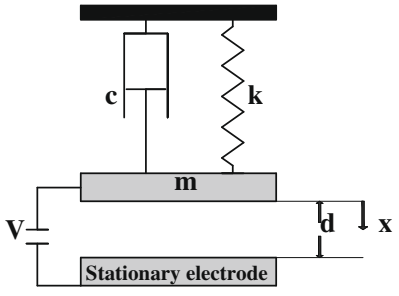

Fig. 1. A single-degree-of-freedom model of a MEMS device.

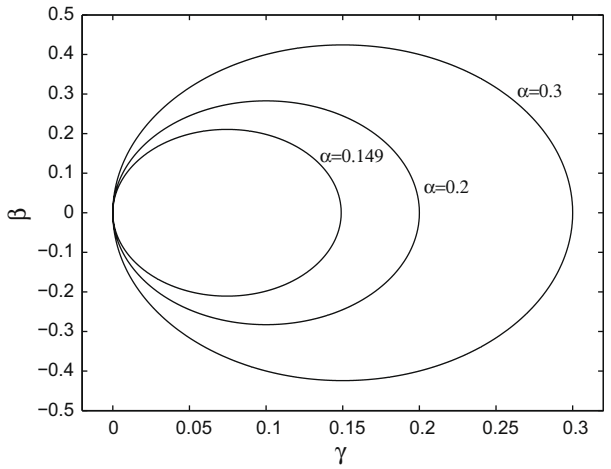

Fig. 2. β versus γ for various values of α.

Indeed, even if the DC voltage V_1 is not introduced, Eqs. (6) and (10) are still valid. The difference is in the definition of the parameters $\alpha,\ \beta$ and γ which are given by

$$\alpha = \frac{\varepsilon A}{2m\omega^2 d^3}\left(V_0^2 + \frac{U^2}{2}\right) \tag{11}$$

$$\beta = \frac{\varepsilon A}{m\omega^2 d^3} V_0 U \tag{12}$$

$$\gamma = \frac{\varepsilon A}{4m\omega^2 d^3} U^2 \tag{13}$$

Eq. (6) contains a slow dynamic which describes the main motions at time-scale of natural vibrations of the microstructure and a fast dynamic at time scale of the high-frequency voltage. To obtain the main equation governing the slow dynamic of the device, we implement the method of direct partition of motion [11] by introducing two different time-scales: a fast time $T_0 = \eta^{-1/2}\tau$ and a slow time $T_1 = \tau$, and we split up the displacement of the mass $X(\tau)$ into a slow part $Z(T_1)$ and a fast part $\phi(T_0, T_1)$ as follows:

$$X(\tau) = Z(T_1) + \phi(T_0, T_1) \equiv Z(T_1) + \eta^2\tilde{\phi}(T_0, T_1) \tag{14}$$

Here the positive parameter η is introduced to measure the smallness of other parameters $(0 < \eta \ll 1)$. As a consequence the high frequency is expressed as $\Omega = \eta^{-1/2}$. The fast motion and its derivatives are assumed to be 2π-periodic functions of the fast time T_0 with zero mean value with respect to it. Thus, $\langle X(\tau)\rangle = Z(T_1)$ where $\langle . \rangle = \frac{1}{2\pi}\int_0^{2\pi}(.)dT_0$ defines the fast time-averaging operator. Introducing $D_m^n = \frac{\partial^n}{\partial T_m^n}$, yields

$$\frac{d}{d\tau} = \eta^{-1/2}D_0 + D_1 \tag{15}$$

$$\frac{d^2}{d\tau^2} = \eta^{-1}D_0^2 + \eta^{-1/2}2D_0D_1 + D_1^2 \tag{16}$$

Substituting Eqs. (15) and (16) into (6) yields to the following equation:

$$\begin{aligned}&\eta(D_0^2\tilde{\phi}) + 2\eta^{3/2}(D_0D_1\tilde{\phi}) + \eta^2(D_1^2\tilde{\phi}) + (D_1^2Z) + 2\xi[\eta^{3/2}(D_0\tilde{\phi}) + \eta^2(D_1\tilde{\phi}) + (D_1Z)] + Z + \eta^2\tilde{\phi}\\ &\quad = \frac{\alpha}{(1 - Z - \eta^2\tilde{\phi})^2} + \frac{\beta}{(1 - Z - \eta^2\tilde{\phi})^2}\cos(T_0) + \frac{\gamma}{(1 - Z - \eta^2\tilde{\phi})^2}\cos(2T_0)\end{aligned} \tag{17}$$

In what follows we set $\beta = \eta\tilde{\beta},\ \gamma = \eta\tilde{\gamma}$ and $\xi = \eta\tilde{\xi}$. The parameters with tildes are of order $O(1)$. The dominant terms depending on T_0 up to the order $O(\eta)$ in Eq. (17) are

$$(D_0^2\tilde{\phi}) = \frac{\tilde{\beta}\cos(T_0)}{(1 - Z)^2} + \frac{\tilde{\gamma}\cos(2T_0)}{(1 - Z)^2} \tag{18}$$

Thus up to this leading order, the fast motion is given by

$$\tilde{\phi}(T_0,T_1) = -\frac{\tilde{\beta}\cos(T_0)}{(1-Z)^2} - \frac{\tilde{\gamma}\cos(2T_0)}{4(1-Z)^2} + O(\eta) \tag{19}$$

Now averaging Eq. (17) over a period of the fast time scale T_0 leads to the following equation:

$$(D_1^2 Z) + 2\xi(D_1 Z) + Z = \left\langle \frac{\alpha}{(1-Z-\eta^2\tilde{\phi})^2} \right\rangle + \left\langle \frac{\beta}{(1-Z-\eta^2\tilde{\phi})^2}\cos(T_0) \right\rangle + \left\langle \frac{\gamma}{(1-Z-\eta^2\tilde{\phi})^2}\cos(2T_0) \right\rangle \tag{20}$$

where up to order $O(\eta^3)$

$$\left\langle \frac{\alpha}{(1-Z-\eta^2\tilde{\phi})^2} \right\rangle = \frac{\alpha}{(1-Z)^2} \tag{21}$$

$$\left\langle \frac{\beta}{(1-Z-\eta^2\tilde{\phi})^2}\cos(T_0) \right\rangle = -\frac{\tilde{\beta}^2}{(1-Z)^5} \tag{22}$$

$$\left\langle \frac{\gamma}{(1-Z-\eta^2\tilde{\phi})^2}\cos(2T_0) \right\rangle = -\frac{\tilde{\gamma}^2}{4(1-Z)^5} \tag{23}$$

Consequently, the equation of the slow dynamics obtained from Eq. (20) can be written as

$$(D_1^2 Z) + 2\xi(D_1 Z) + Z = \frac{\alpha}{(1-Z)^2} - \frac{4\beta^2+\gamma^2}{4\Omega^2(1-Z)^5} \tag{24}$$

The last term of the right hand side of Eq. (24) is the effect of the HFV on the slow motion of the mass. It is worth noting that the zeros of the slow dynamic (24) are the averaged positions around which the periodic solutions of Eq. (6) oscillate. To obtain these fixed points the following sixth order algebraic equation should be solved:

$$Z(1-Z)^5 = \alpha(1-Z)^3 - \frac{4\beta^2+\gamma^2}{4\Omega^2} \tag{25}$$

For $\beta = 0$ and $\gamma = 0$ the standard case of the static tension is obtained i.e., $Z(1-Z)^2 = \alpha$. The static pull-in in this case is given by $\alpha_p = \frac{4}{27}$ which corresponds to the steady state displacement $Z_p = \frac{1}{3}$.

Up to the order $O(\eta^3)$, the solution of Eq. (6) is given by

$$X(\tau) = Z - \frac{\beta\cos(\Omega\tau)}{\Omega^2(1-Z)^2} - \frac{\gamma\cos(2\Omega\tau)}{4\Omega^2(1-Z)^2} + O(\eta^3) \tag{26}$$

3. Pull-in suppression

In this section, we analyze the effect of HFV on the suppression of the pull-in instability using the slow dynamic Eq. (24) and numerical simulations of Eq. (6) using Runge–Kutta method . We begin by analyzing the response of the system to a DC voltage in the absence of AC voltage i.e., $\beta = 0$. The damping coefficient is taken $\xi = 0.01$ in all computations. In Fig. 3, the

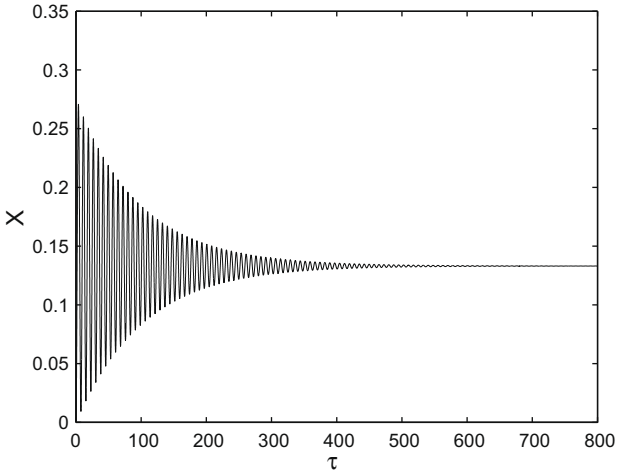

Fig. 3. Time history of Eq. (6) for $\alpha = 0.1$, and $\beta = 0,\ \gamma = 0$.

normalized displacement to the gap $X(\tau)$ is shown for $\alpha = 0.1$. We note that the steady-state amplitude is near $X = 0.133$. In Fig. 4, the time history of Eq. (6) is shown for $\alpha = 0.15$ which corresponds to a post pull-in threshold value. This instability is characterized by the slope of the displacement approaching infinity.

The effect of the HFV on the pull-in instability is studied in the case where the mass is in the post pull-in state caused by an electrostatic force $\alpha = 0.15$ (see Fig. 4). The shift of the averaged solution from the zero solution are computed using the following relation:

$$shift = \frac{\max(X(\tau)) + \min(X(\tau))}{2} \tag{27}$$

Fig. 5 shows, for $\Omega = 7$, the stationary solutions Z of the slow dynamic (25) and the shift of the averaged solutions of Eq. (6) versus the amplitude γ of the HFV. It can be seen that the HFV creates a stable position in the safe range i.e., $X < 1$. This figure shows that it is possible to suppress the pull-in for $\gamma \in [0.0269, 0.1279]$.

In Fig. 6, the quasi-static solutions given by Eq. (25) (lines) and the averaged positions of Eq. (6) (circles) are shown versus Ω for $\gamma = 0.1$. For $\Omega < 9$, there is one stable solution in the range $Z < 1/3$ which disappears by a saddle-node bifurcation. In Fig. 7 is shown the good agreement between the numerical solution of Eq. (6) and the analytical solution (26) validating the used approach.

Fig. 8 shows in the plane of the frequency and amplitude of the HFV (Ω, γ) the zone where the electrostatically induced pull-in instability can be suppressed (the grey zone). The grey zone is becoming larger, in terms of the amplitude of the HFV

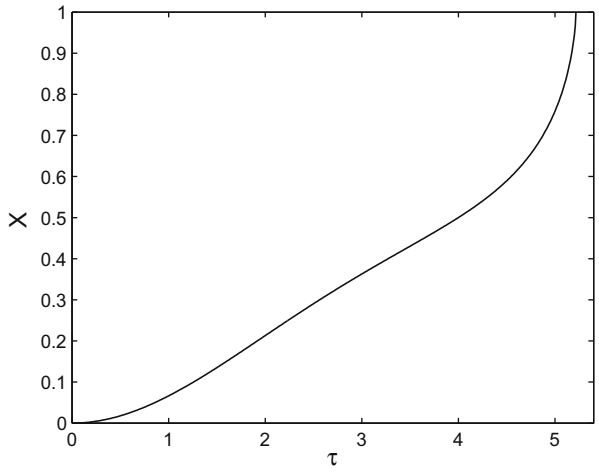

Fig. 4. Time history of Eq. (6) for $\alpha = 0.15$, and $\beta = 0,\ \gamma = 0$.

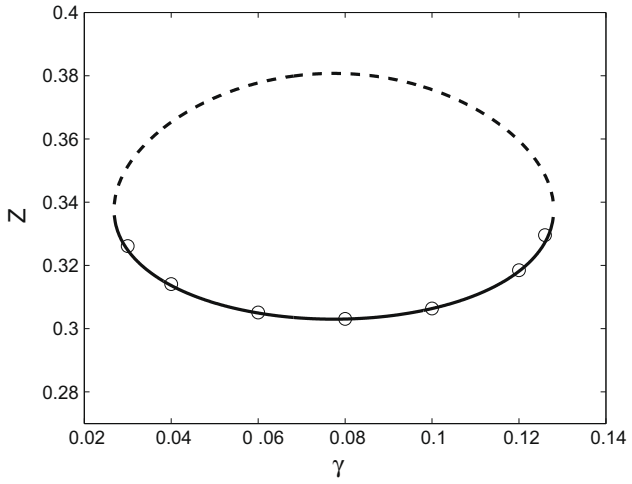

Fig. 5. The averaged position of vibration versus γ for $\Omega = 7$ and $\alpha = 0.15$: (○) numerical integration of Eq. (6). Zeros of Eq. (25): (–) stable and (--) unstable.

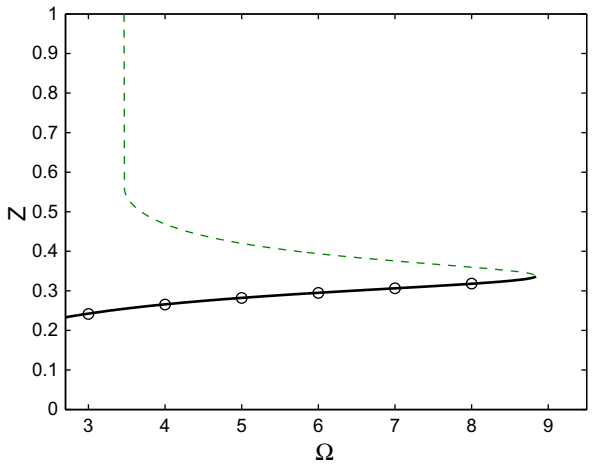

Fig. 6. The averaged position of vibration versus Ω for $\gamma = 0.1$ and $\alpha = 0.15$. Numerical integration of Eq. (6): (○) numerical integration of Eq. (6). Zeros of Eq. (25): (–) stable and (--) unstable.

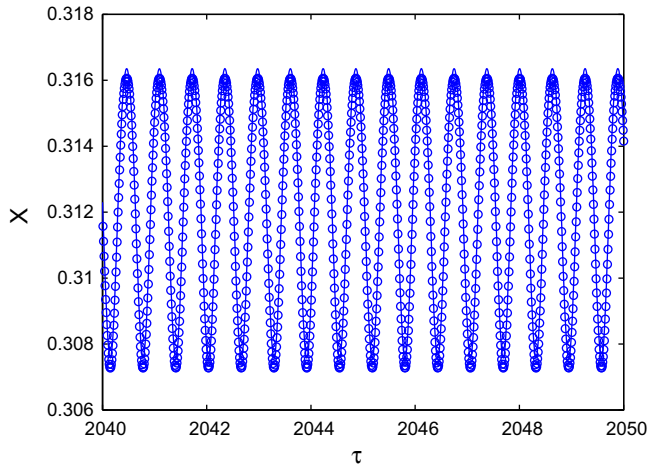

Fig. 7. Time history of Eq. (6) for $\alpha = 0.149,\ \Omega = 10$ and $\gamma = 0.0624$: (○) Numerical integration of Eq. (6) and lines analytical solution (26).

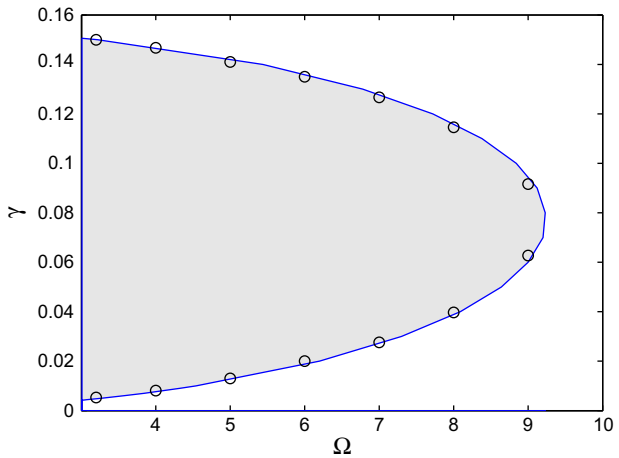

Fig. 8. Suppression zone of the pull-in instability in the plane (Ω, γ) for $\alpha = 0.15$: lines using Eq. (25) and (○) using Eq. (6).

γ, for decreasing Ω. Note that our results are valid only for $\Omega = O(\eta^{-1/2})$ which means that we can not continue to decrease Ω lower than 3.

Based on the previous results, we claim that the static pull-in of a clamped-clamped microbeam, made of Silicon and investigated in [9], can be suppressed using an adequate HF voltage. The geometric parameters of the microbeam are as follows: the length is $L = 510$ μm, the thickness is $h = 1.5$ μm, the width is $b = 100$ μm and the gap width is $d = 1.18$ μm. The natural frequency of the microstructure is 50 kHz. The static pull-in voltage is $V_{dc} = 4.357$ V. This pull-in voltage corresponds to $\alpha = 4/27$. For a DC voltage $V_{dc} = 4.384$ V the system is in the post pull-in state. If we add a high-frequency actuation with $\Omega = 8$ which is equivalent to a frequency 400 kHz, and for an amplitude of the HFV, $\gamma \in [0.0397, 0.1146]$ corresponding to $U \in [3.19\text{ V}, 5.42\text{ V}]$, the static pull-in instability can be suppressed.

4. Conclusion

The effect of a high-frequency actuation on the suppression of the static pull-in instability is studied analytically and numerically in this paper. A one dimensional lumped model was considered and the main equation governing the slow dynamic of the microstructure is derived by applying an averaging technique. The influence of the high-frequency AC actuation on the pull-in phenomenon is investigated by analyzing the fixed points of the slow dynamic. It was shown that when the microstructure is in the pull-in instability situation, adding a high-frequency AC actuation can create a new attracting solution which can avoid the failure of the device. This result indicates that by implementing a HFV, pull-in instability can be prevented in capacitive MEMS operating in regimes with relatively large amplitude. Taking advantage of this result, current efforts are directed analytically and numerically to control and suppress undesirable nonlinear characteristics in MEMS as dynamic pull-in and hysteresis.

References

[1] Osterberg P. Electrostatically actuated microelectromechanical test structures for material property measurement. PhD thesis, MIT; 1995.
[2] Younis MI, Abdel-Rahman EM, Nayfeh AH. Static and dynamic behavior of an electrically excited resonant microbeam. In: Proceedings of the 43rd AIAA structures, structural dynamics, and materials conference. Denver,CO, AIAA Paper, 20021305; 2002.
[3] Abdel-Rahman EM, Younis MI, Nayfeh AH. A nonlinear reduced-order model for electrostatic MEMS. In: Proceedings of the 19th biennial conference in mechanical vibration and noise (VIB). Chicago, IL, Paper DETC2003/VIB-48517; 2003.
[4] Walraven JA. Future challenges for MEMS failure analysis. In: Proceedings of ITC international test conference, paper 33.4; 2003. p. 850–5.
[5] Abdel-Rahman EM, Younis MI, Nayfeh AH. Characterization of the mechanical behavior of an electrically actuated microbeam. J Micromech Microeng 2002;12:766–95.
[6] Tilmans HA, Legtenberg R. Electrostatically driven vacuum-encapsulated polysilicon resonators. Part II: theory and performance. Sensors Actuators A 1994;45:6784.
[7] Krylov S, Maimon R. Pull-in dynamics of an elastic beam actuated by distributed electrostatic force. In: Proceedings of ASME design eng. tech. conf., Chicago, USA, 2–6 September (paper DETC2003/Vib-48518); 2003.
[8] Nayfeh AH, Younis MI, Abdel-Rahman EM. Dynamic pull-in phenomenon in MEMS resonators. Nonlinear Dyn 2007;48:153–63.
[9] Younis MI, Miles R, Jordy D. Investigation of the response of microstructures under the combined effect of mechanical shock and electrostatic forces. J Micromech Microeng 2006;16:2463–74.
[10] Lenci S, Rega G. Control of pull-in dynamics in a nonlinear thermoelastic electrically actuated microbeam. J Micromech Microeng 2006;16:390–401.
[11] Thomsen JJ. Vibrations and stability: advanced theory, analysis, and tools. Berlin-Heidelberg: Springer-Verlag; 2003.
[12] Thomsen JJ. Some general effects of strong high-frequency excitation: stiffening, biasing, and smoothening. J Sound Vibr 2002;253:807–31.
[13] Thomsen JJ. Slow high-frequency effects in mechanics: problems, solutions, potentials. Int J Bifurcation Chaos 2005;15(9):2799–818.
[14] Mann BP, Koplow MA. Symmetry breaking bifurcations of a parametrically excited pendulum. Nonlinear Dyn 2006;46:427–37.
[15] Bourkha M, Belhaq M. Effect of vertical high-frequency parametric excitation on self-excited motion in a delayed van der Pol oscillator. Chaos Solitons Fractals 2008;37:1489–96.
[16] Belhaq M, Fahsi A. 2:1 and 1:1 frequency-locking in fast excited van der Pol-Mathieu–Duffing oscillator. Nonlinear Dyn 2008;53:139–52.
[17] Belhaq M, Fahsi A. Hysteresis suppression for primary and subharmonic 3:1 resonances using fast excitation. Nonlinear Dyn 2009;57:275–87.